Citation: Molecular Therapy—Nucleic Acids (2013) 2, e124; doi:10.1038/mtna.2013.51

www.nature.com/mtna

Context Dependent Effects of Chimeric Peptide Morpholino Conjugates Contribute to Dystrophin Exon-skipping Efficiency

HaiFang Yin[1,2], Prisca Boisguerin[3], Hong M Moulton[4], Corinne Betts[2], Yiqi Seow[2], Jordan Boutilier[5], Qingsong Wang[1], Anthony Walsh[2], Bernard Lebleu[3] and Matthew JA Wood[2]

We have recently reported that cell-penetrating peptides (CPPs) and novel chimeric peptides containing CPP (referred as B peptide) and muscle-targeting peptide (referred as MSP) motifs significantly improve the systemic exon-skipping activity of morpholino phosphorodiamidate oligomers (PMOs) in dystrophin-deficient *mdx* mice. In the present study, the general mechanistic significance of the chimeric peptide configuration on the activity and tissue uptake of peptide conjugated PMOs *in vivo* was investigated. Four additional chimeric peptide-PMO conjugates including newly identified peptide 9 (B-9-PMO and 9-B-PMO) and control peptide 3 (B-3-PMO and 3-B-PMO) were tested in *mdx* mice. Immunohistochemical staining, RT-PCR and western blot results indicated that B-9-PMO induced significantly higher level of exon skipping and dystrophin restoration than its counterpart (9-B-PMO), further corroborating the notion that the activity of chimeric peptide-PMO conjugates is dependent on relative position of the tissue-targeting peptide motif within the chimeric peptide with respect to PMOs. Subsequent mechanistic studies showed that enhanced cellular uptake of B-MSP-PMO into muscle cells leads to increased exon-skipping activity in comparison with MSP-B-PMO. Surprisingly, further evidence showed that the uptake of chimeric peptide-PMO conjugates of both orientations (B-MSP-PMO and MSP-B-PMO) was ATP- and temperature-dependent and also partially mediated by heparan sulfate proteoglycans (HSPG), indicating that endocytosis is likely the main uptake pathway for both chimeric peptide-PMO conjugates. Collectively, our data demonstrate that peptide orientation in chimeric peptides is an important parameter that determines cellular uptake and activity when conjugated directly to oligonucleotides. These observations provide insight into the design of improved cell targeting compounds for future therapeutics studies.

Molecular Therapy—Nucleic Acids (2013) **2**, e124; doi:10.1038/mtna.2013.51; published online 24 September 2013
Subject Category: Nucleic acid chemistries Antisense oligonucleotides

Introduction

Duchenne muscular dystrophy (DMD) is a severe muscle degenerative disease caused primarily by mutations in the dystrophin gene that result in an out-of-frame transcript, producing an unstable nonfunctional dystrophin protein. Skipping of nonessential exons, induced by antisense oligonucleotides (AOs), can restore the reading-frame and generate a truncated, but semi-functional dystrophin protein with compatible functional improvement.[1] AO-mediated exon-skipping therapies have recently shown great promise in animal models of DMD[2–5] and therapeutic potential in human subjects.[6,7]

Numerous studies have been undertaken to investigate improved or novel AOs for exon skipping in DMD in the past two decades. Phosphorodiamidate morpholino oligomers (PMOs) are currently one of the effective types of AOs for inducing exon-skipping in DMD patients.[7] Systemic intravenous delivery of PMOs has been shown to restore dystrophin expression in multiple peripheral muscles in the dystrophin-deficient *mdx* mouse, which contains a premature stop codon in exon 23.[3] However, much like other chemistries utilized,[2,8] systemic correction was of relatively low efficiency and in the case of PMOs required a multiple-dosing regimen comprising seven weekly doses of 100 mg/kg[3] or a single large dose of 3 g/kg[9] with no or limited effect in heart.

Recently, we and others have reported that PMOs conjugated to short arginine-rich cell-penetrating peptides (CPPs) can induce effective systemic dystrophin exon skipping, including in cardiac muscle,[5,10–12] highlighting the potential of such peptide conjugates to improve delivery efficacy for the treatment of DMD. Furthermore, utilizing a chimeric fusion peptide composed of a muscle-specific heptapeptide (MSP)[13] and a CPP (henceforth referred as B peptide),[10,11] directly conjugated to 5′ end of PMOs, showed highly effective systemic dystrophin splice correction in *mdx* mice at low systemic doses.[14,15] Importantly, treatment with such peptide-PMO conjugates led to body-wide restoration of dystrophin protein and functional correction in *mdx* mice with no evidence of toxicity. Interestingly, the effectiveness of this chimeric peptide-PMO conjugate appeared to depend on the

[1]Research Centre of Basic Medical Science, Tianjin Medical University, Qixiangtai Road, Heping District, Tianjin, China; [2]Department of Physiology, Anatomy and Genetics, University of Oxford, South Parks Road, Oxford, UK; [3]UMR 5235 CNRS, Dynamique des Interactions Membranaires Normales et Pathologiques, Université Montpellier 2, Montpellier Cedex 5, France; [4]Biomedical Sciences, College of Veterinary Medicine, Oregon State University, Corvallis, Oregon, USA; [5]Siga Labs, 4575 SW Research Way, Suite 230, Corvallis, Oregon, USA. Correspondence: Dr HaiFang Yin, Research Centre of Basic Medical Science, Tianjin Medical University, Qixiangtai Road, Heping District, Tianjin, 300070, China. E-mail: haifangyin@tmu.edu.cn or Matthew JA Wood, Department of Physiology, Anatomy and Genetics, University of Oxford, South Parks Road, Oxford, OX1 3QX, UK. E-mail: matthew.wood@dpag.ox.ac.uk
Keywords: antisense oligonucleotide; chimeric peptide conjugate; Duchenne muscular dystrophy; exon skipping
Received 20 May 2013; accepted 16 July 2013; advance online publication 24 September 2013. doi:10.1038/mtna.2013.51

peptide motif orientation with B-MSP-PMO being significantly more effective than MSP-B-PMO.

In order to elucidate the mechanism by which the B-MSP chimeric peptide conferred enhanced cell uptake and improved systemic exon-skipping activity, we have now undertaken studies to investigate the activity and cell uptake properties of the chimeric peptide PMO conjugates in detail. We now demonstrate that the increased exon-skipping activity conferred by the chimeric peptide is order and sequence-dependent. Moreover, we demonstrate the general significance of this observation by replacing MSP with an alternative muscle-targeting peptide or with a non-muscle targeting control peptide. Further, we show that the increased exon-skipping efficacy of B-MSP-PMO over MSP-B-PMO can largely be attributed to increased muscle cell uptake. Finally, we demonstrate that the cell uptake of both B-MSP-PMO and MSP-B-PMO is energy and temperature-dependent, implying that cell uptake is likely to be mediated by endocytosis, and additionally that interaction with surface heparan sulfate proteoglycans (HSPG) is also important. These results provide insight into the mechanisms of action and design of future tissue-targeting/cell-penetrating chimeric peptide conjugates for enhancing the cellular delivery of oligonucleotides and demonstrate the potential of these chimeric peptide conjugates for exon-skipping treatment of DMD.

Results

Chimeric peptide-PMO activity is dependent on relative peptide motif order with respect to PMO

We have previously demonstrated that the efficacy of an exon-skipping PMO conjugated to a chimeric peptide consisting of the B peptide and a muscle-targeting peptide (MSP) is dependent upon the orientation of these peptides with respect to PMO, with B-MSP-PMO being significantly more effective than MSP-B-PMO.[14] To investigate the general significance of this observation, we replaced MSP with another muscle-targeting peptide, peptide 9, identified through an *in vivo* phage display screen and shown to have strong binding affinity to muscle and heart tissues[15] (**Table 1**, **Figure 1a**). Body-wide muscles including the heart were evaluated for the efficiency of exon-skipping following a single intravenous injection of either B-9-PMO or 9-B-PMO in adult *mdx* mice at 25 mg/kg doses. Up to 100% dystrophin-positive fibers were detected in tibialis anterior, quadriceps, biceps, and abdominal muscle cross-sections with B-9-PMO treatment as shown by immunohistochemical staining, whereas a significantly lower level of dystrophin expression was observed in the corresponding muscles treated with 9-B-PMO (**Figure 1b**,**c**). No detectable unskipped dystrophin transcript was observed in any peripheral muscles treated with B-9-PMO, and much greater exon skipping was detected at the RNA level even in heart compared with that of 9-B-PMO (**Figure 1d**). Up to 100% of total dystrophin protein was restored in peripheral muscles treated with B-9-PMO and about 20% of normal levels of dystrophin protein restored in heart as determined by western blot (**Figure 1e**). In contrast, 9-B-PMO demonstrated a significantly reduced activity in all muscles in comparable assays. This result is consistent with our previous report identifying B-MSP-PMO and supports the hypothesis that the activity of chimeric peptide-PMO conjugates is dependent on alignment of the tissue-specific peptide with respect to the arginine-rich domain and the PMO sequence, with B-MSP-PMO and now B-9-PMO having significantly enhanced activity compared with the reverse order of chimeric peptide-PMO conjugates.

In line with the above observations, no enhanced exon-skipping activity could be detected when a nonmuscle targeting control peptide, derived from our phage display screen as a negative control and showing no binding affinity with muscle and heart[16] (**Table 1**), was inserted into the chimeric peptide, in place of MSP. Consistently, compared with B-PMO as we reported earlier,[14] this nonmuscle targeting control chimeric peptide-PMO conjugate was less effective than B-PMO in either orientation (**Supplementary Figure 1**, online), suggesting that the addition of nonmuscle targeting peptides partially negated the cell-penetrating property of the B peptide, which is likely due to the steric hindrance caused by the additional nonmuscle targeting peptide by preventing effective membrane contact of the CPP moiety.

Peptide configuration affects PMO tissue uptake *in vivo*

The remarkable restoration of dystrophin with chimeric peptide-PMO conjugates could be due to either increased PMO uptake or a direct influence of the conjugated peptides on exon-skipping efficiency. Thus, B-MSP-PMO and MSP-B-PMO were labeled with fluorescein at the 3′ end of the PMO and were administered into adult *mdx* mice by single intravenous injection at 25 mg/kg dose. Body-wide muscle tissues including tibialis anterior, quadriceps, gastrocnemius, biceps, diaphragm, heart, abdominal muscle, liver and kidney, spleen were harvested 10 days after administration and exon-skipping efficiency evaluated in all peripheral muscles and heart by immunohistochemical staining, RT-PCR and western blot (**Figure 2a**–**d**). The results indicated that the fluorescein-labeled peptide-PMO conjugates were readily taken up by muscle cells and that the modification with fluorescein did not affect the exon-skipping activity of PMO. Consistently, B-MSP-PMO showed superior activity to MSP-B-PMO in restoring dystrophin expression as reported previously.[14] To investigate whether the improved activity of B-MSP-PMO was due to enhanced cellular uptake or to other factors, we quantified the content of fluorescein-labeled peptide-PMO conjugates in various tissues by homogenizing the tissues and extracting labeled compounds with the digestion buffer containing proteinase. The samples were then assayed against a standard curve derived from known

Table 1 Oligonucleotide and peptide nomenclature and sequences

Name	Sequence	Abbreviation	Length
M23D	5′-GGCCAAACCTCGGCTTACC TGAAAT-3′	PMO	25
B peptide	N- RXRRBRRXRRBRXB –C	$(RXRRBR)_2XB$	14
3 peptide	N- IVHPSTMX- C	3	7
9 peptide	N- SKTFNTHPQSTPX- C	9	12

B, β-alanine; PMO, phosphorodiamidate oligomers; X, 6-aminohexanoic acid.

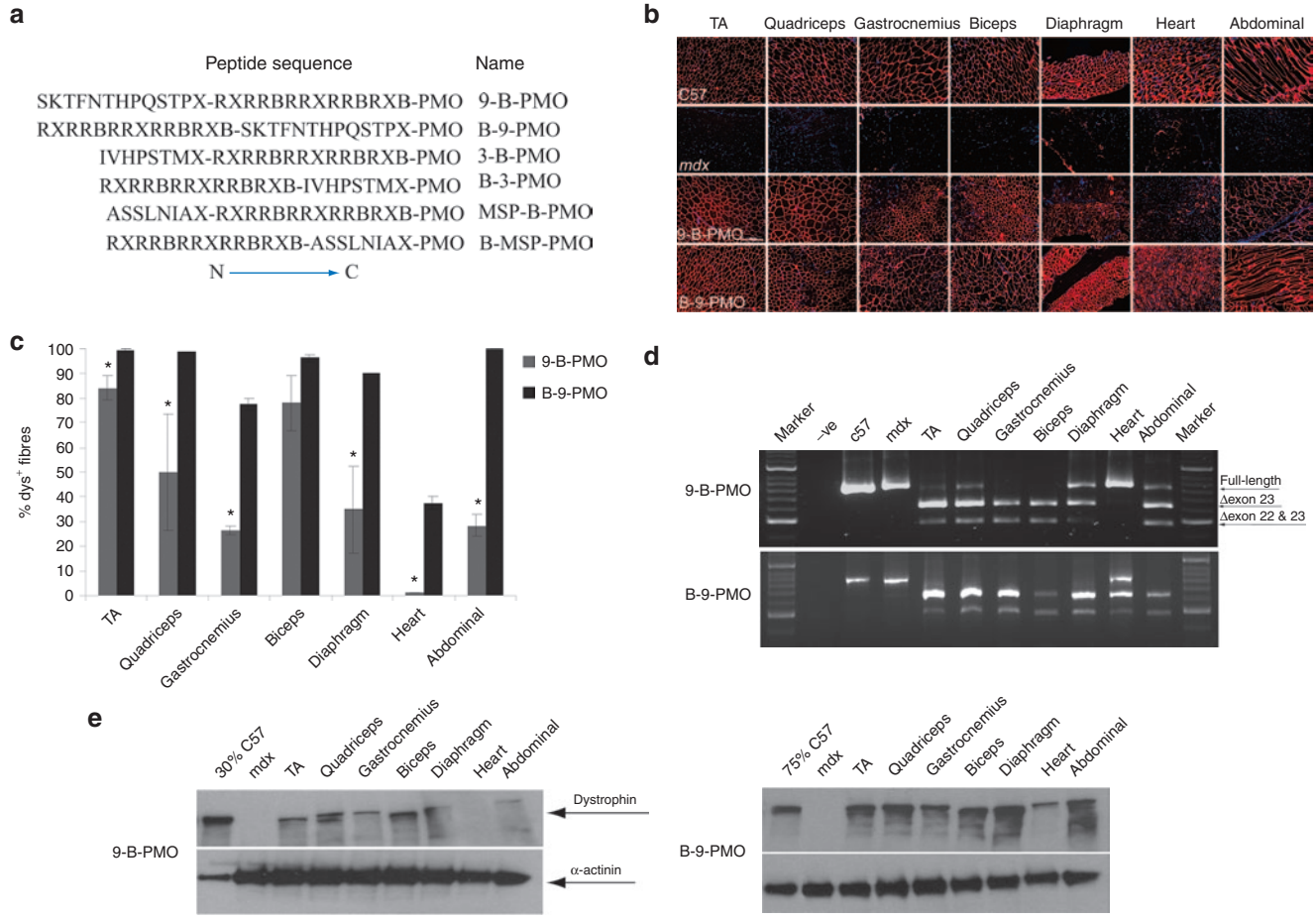

Figure 1 Systemic administration of 9-B-PMO and B-9-PMO conjugates in adult *mdx* mice. Dystrophin expression following single 25 mg/kg intravenous injections of the 9-B-PMO and B-9-PMO conjugates in young adult *mdx* mice. (**a**) Schematic figure illustrating the six different AO constructs utilized. PMO contains the sequence of GGCCAAACCTCGGCTTACCTGAAAT (5′–3′). Peptides are written from N to C orientation using the standard one letter amino acid code except for X and B, which are un-natural amino acids (X, 6-aminohexanoic acid, B, β-alanine). (**b**) Immunostaining of muscle tissue cross-sections to detect dystrophin protein expression and localization in C57BL/6 normal control (top panel), untreated *mdx* mice (second panel), 9-B-PMO treated (third panel) and B-9-PMO treated *mdx* mice (bottom panel). Muscle tissues analyzed were from tibialis anterior (TA), gastrocnemius, quadriceps, biceps, diaphragm, heart, and abdominal wall (abdominal) muscles (scale bar: 200 µm). (**c**) Quantification of dystrophin-positive fibers in muscle cross-sections from *mdx* mice treated with 25 mg/kg 9-B-PMO and B-9-PMO. The data is presented as mean ± SEM and significant difference was observed in B-9-PMO treated *mdx* mice compared with 9-B-PMO (*t*-test, $^*P < 0.05$; $n = 4$, *n* represents the number of biological replicates). (**d**) RT-PCR to detect exon-skipping efficiency at the RNA level. Exon-skipping products are shown by shorter exon-skipped bands (indicated by Δexon23 – exon 23 deleted; Δexon22&23 – both exon 22 and 23 skipped). (**e**) Western blot for dystrophin expression in 9-B-PMO and B-9-PMO treated *mdx* mice. Equal loading of 10-µg protein is shown for each sample except for the C57BL/6 control lanes where 5 and 2.5 µg protein was loaded, respectively. α-actinin was used as loading control. There was no visible difference in the size of dystrophins between muscle treated with peptide-PMO conjugates and muscle from the normal C57BL/6 mouse. AO, antisense oligonucleotides; MSP, muscle-targeting peptide; PMO, phosphorodiamidate oligomers.

concentrations of identical fluorescein-labeled conjugates, using untreated control *mdx* mouse tissues for background normalization. A significantly greater amount of fluorescence was detected in several muscle tissues treated with B-MSP-PMO when compared with those treated with MSP-B-PMO (**Figure 2e**), suggesting that increased cellular uptake and/or retention of B-MSP-PMO in tissues is directly responsible for the difference in exon-skipping activity observed and in the resulting dystrophin protein restoration. Interestingly, higher uptake was observed for B-MSP-PMO in heart, which is the tissue with the lowest exon-skipping efficiency compared with other skeletal muscles as shown in **Figure 2d**,**e**, implying that the enhanced penetration property conferred by B peptide resulted in increased uptake in heart, but probably only a fraction of these traffic into the nuclei, where the compounds are required for functional effects, as shown in our previous study with Pip5e-PMO.[17] Although the majority of fluorescein-labeled peptide-PMO conjugates were localized in nonmuscle tissues that is, liver and kidney, from the tissue distribution analysis (**Figure 2e**) there was less B-MSP-PMO conjugate detected in these nonmuscle tissues than MSP-B-PMO, suggesting that the chimeric B-MSP peptide conferred a degree of preferential muscle targeting. For the undetectable level of MSP-B-PMO conjugates in some skeletal muscles e.g., biceps, gastrocnemius, and quadriceps, it is likely due to the limited sensitivity of current test system as the level of B-MSP-PMO conjugates was also very low in these corresponding tissues.

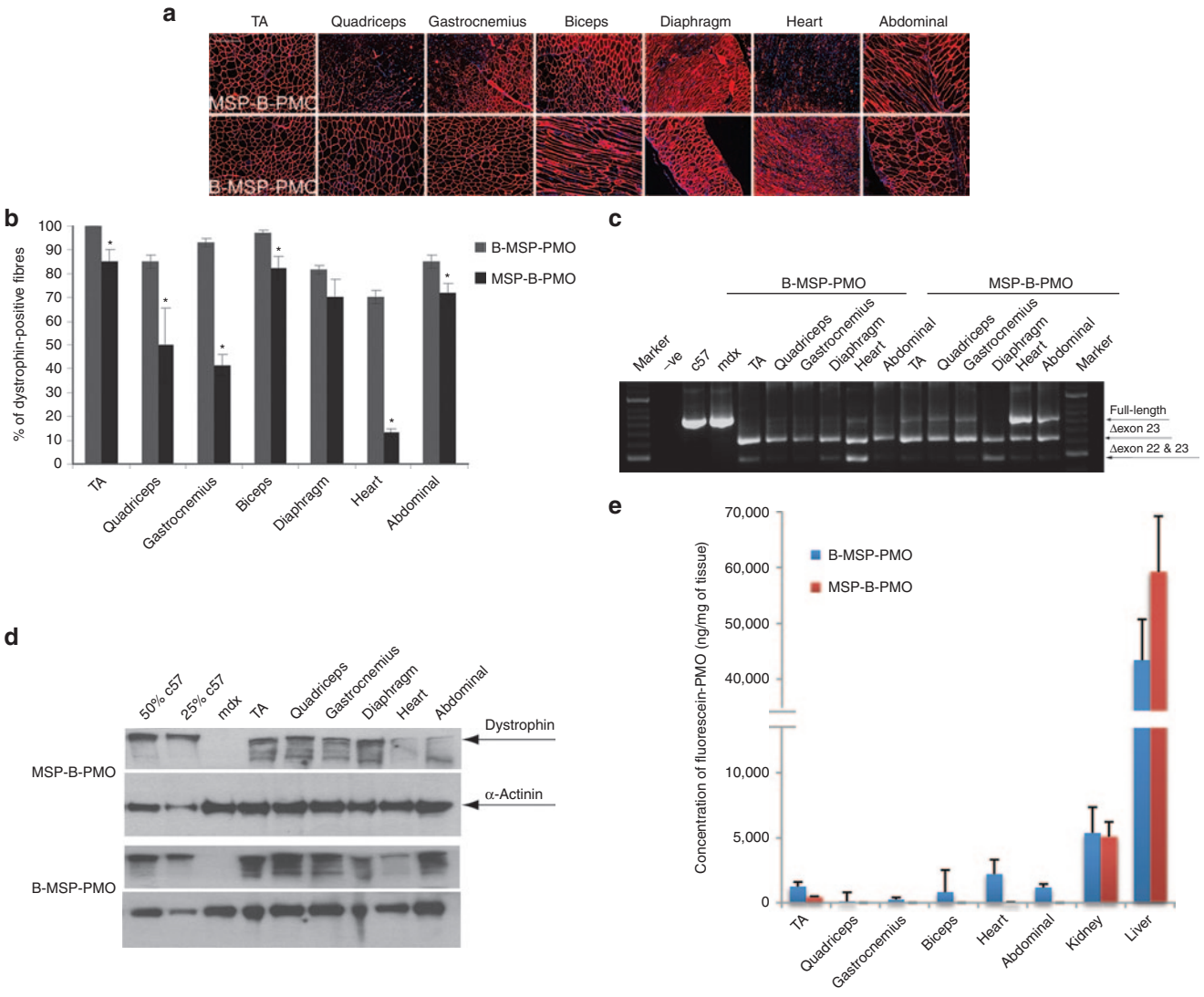

Figure 2 Correlation between the exon-skipping efficacy and tissue distribution for fluorescence-labeled B-MSP-PMO and MSP-B-PMO. Dystrophin expression and quantification of cellular uptake in body-wide muscles following systemic intravenous administration of fluorescence-labeled B-MSP-PMO and MSP-B-PMO at 25 mg/kg dose. (**a**) Immunostaining of muscle tissue cross-sections to detect dystrophin protein expression and localization in fluorescence-labeled MSP-B-PMO treated (top panel) and B-MSP-PMO treated *mdx* mice (bottom panel). Muscle tissues analyzed were from tibialis anterior (TA), gastrocnemius, quadriceps, biceps, diaphragm, heart, and abdominal wall (abdominal) muscles (scale bar: 200 µm). (**b**) Quantification of dystrophin-positive fibers in muscle cross-sections from *mdx* mice treated with 25 mg/kg fluorescence-labeled MSP-B-PMO and B-MSP-PMO. The data is presented as mean ± SEM and significant difference was detected in labeled B-MSP-PMO samples compared with MSP-B-PMO (*t*-test, $^*P < 0.05$; $n = 4$, n represents the number of biological replicates). (**c**) RT-PCR to detect exon-skipping efficiency at the RNA level. Exon-skipping products are shown by shorter exon-skipped bands (indicated by Δexon23 – exon 23 deleted; Δexon22&23 – both exon 22 and 23 skipped). (**d**) Western blot for dystrophin expression in MSP-B-PMO and B-MSP-PMO treated *mdx* mice. Equal loading of 10-µg protein is shown for each sample except for the C57BL/6 control lanes where 5 and 2.5 µg protein was loaded. (**e**) Tissue distribution data fluorescence for fluorescence-labeled B-MSP-PMO and MSP-B-PMO in body-wide muscles following single systemic intravenous injection of 25 mg/kg florescence-labeled compounds. Substantially increased uptake in muscle groups treated with B-MSP-PMO compared with corresponding tissues treated with MSP-B-PMO was observed (*t*-test, $^*P < 0.05$; $n = 4$, n represents the number of biological replicates). MSP, muscle-targeting peptide; PMO, phosphorodiamidate oligomers.

Enhanced cellular uptake of B-MSP-PMO into muscle cells leads to increased exon-skipping activity

From the above *in vivo* tissue distribution study, a clear relationship was observed between the increased muscle cell uptake and improved exon-skipping activity observed with chimeric peptide-PMO compounds such as B-MSP-PMO. In order to ascertain if the increased exon skipping was dependent on increased uptake of PMO into muscle cells, fluorescein-labeled B-MSP-PMO and MSP-B-PMO conjugates were applied to H2K *mdx* myoblasts *in vitro*.[8] Confocal microscopy was utilized to monitor the localization of the fluorescein-labeled peptide-PMO conjugates. Interestingly, both conjugates were taken up by H2K *mdx* cells at the concentration of 1 µmol/l and localized to discrete intracellular foci (**Figure 3a**), albeit to a significantly lesser extent with MSP-B-PMO. Quantification of cell uptake of both peptide-PMO

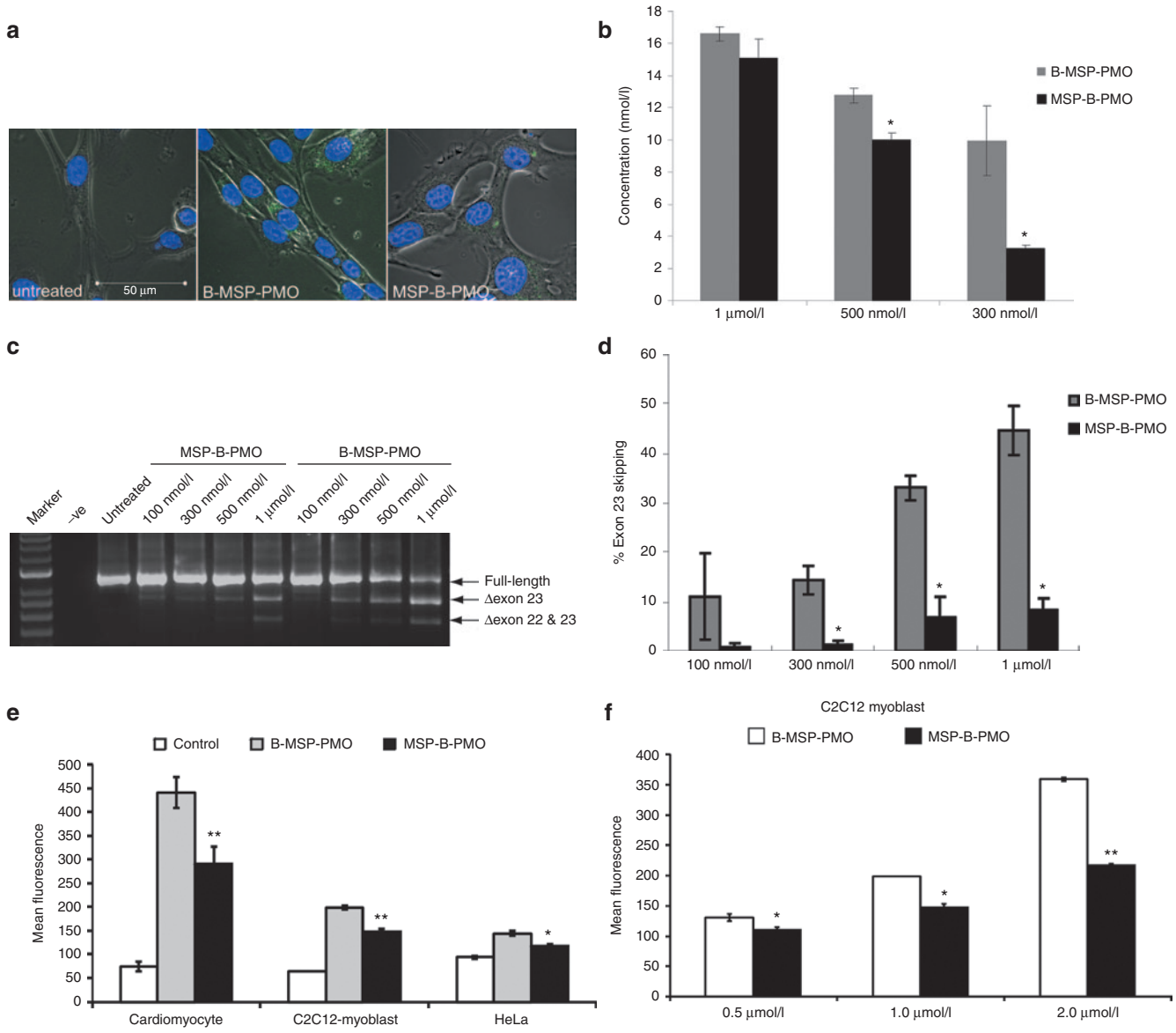

Figure 3 Enhanced exon-skipping activity is due to increased cellular internalization. Localization and quantification of fluorescence-labeled conjugates in H2K *mdx* cells. (**a**) Confocal microscopic image of fluorescence-labeled conjugates at 1 µmol/l in H2K *mdx* cells. The data show greater nuclear colocalization was observed with B-MSP-PMO than with MSP-B-PMO (scale bar: 50 µm), blue is nuclei staining with Hoechst and green refers to FITC-labeled peptide-PMO conjugates. (**b**) Measurement of total cellular uptake with fluorescence-labeled conjugates at different concentrations with fluorescence plate-reader. The data shows mean ± SEM and significantly higher uptake is detected with B-MSP-PMO than MSP-B-PMO at 300 and 500 nmol/l (*t*-test, $^*P < 0.05$; $n = 6$, *n* represents the number of biological replicates). (**c**) RT-PCR to detect the efficiency of exon skipping at the RNA level. Exon-skipping products are shown by shorter exon-skipped bands (indicated by Δexon23 – exon 23 deleted; Δexon22&23 – both exon 22 and 23 skipped). (**d**) Quantification of the efficiency of exon skipping at the RNA level in H2K *mdx* cells. The data is presented as mean ± SEM and significantly higher exon-skipping activity was detected with B-MSP-PMO than MSP-B-PMO at 300 nmol/l, 500 nmol/l and 1 µmol/l (*t*-test, $^*P < 0.05$; $n = 6$, *n* represents the number of biological replicates). (**e**) Cellular uptake study for fluorescence-labeled peptide-PMO conjugates in different cell types. Fluorescence-labeled B-MSP-PMO and MSP-B-PMO were tested in different cell types i.e., primary mouse cardiomyocytes ($^{**}P < 0.001$ means significant difference between B-MSP-PMO and MSP-B-PMO), C2C12 myoblasts ($^{**}P < 0.001$ means significant difference between B-MSP-PMO and MSP-B-PMO; $^*P < 0.05$ refers to significant difference between B-MSP-PMO) and HeLa cells ($^*P < 0.05$ refers to significant difference between B-MSP-PMO and MSP-B-PMO) at different concentrations. The graph illustrates certain degree of muscle preference with B-MSP-PMO conjugate compared with other peptide conjugates and the highest uptake was observed with fluorescence-labeled B-MSP-PMO in all the tested cells. (**f**) Quantification of cellular uptake with fluorescence-labeled B-MSP-PMO and MSP-B-PMO in C2C12 myoblast at 0.5 µmol/l ($^*P < 0.05$ refers to significant difference between B-MSP-PMO and MSP-B-PMO), 1 µmol/l ($^*P < 0.05$ refers to significant difference between B-MSP-PMO and MSP-B-PMO), 2 µmol/l ($^{**}P < 0.001$ refers to significant difference between B-MSP-PMO and MSP-B-PMO; $^*P < 0.01$ means significance between B-MSP-PMO). The data is presented as mean ± SEM ($n = 6$, *n* represents the number of biological replicates) and shows dose-dependent increased uptake. MSP, muscle-targeting peptide; PMO, phosphorodiamidate oligomers.

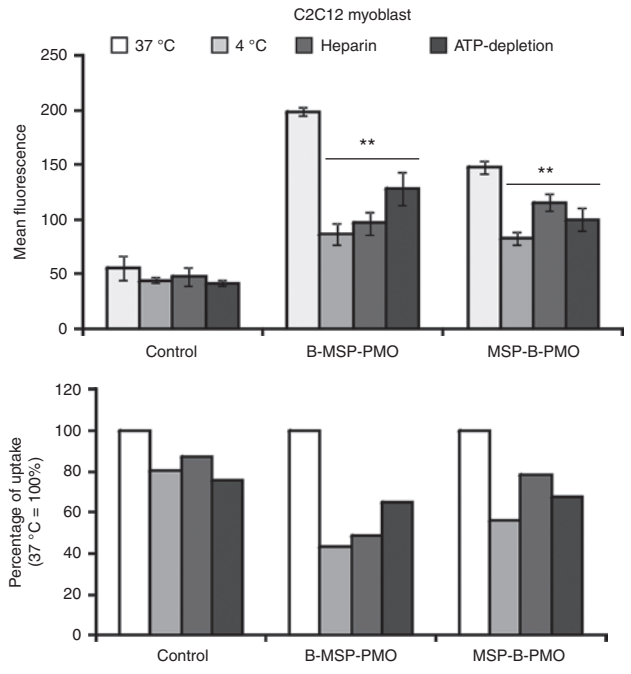

Figure 4 Identification of uptake pathway for fluorescence-labeled B-MSP-PMO and MSP-B-PMO conjugates in C2C12 myoblast. Cellular uptake of fluorescence-labeled peptide-PMO conjugates is inhibited at 4 °C and by depletion of cellular ATP in C2C12 myoblast. Involvement of heparan sulfate receptors in the cellular uptake of fluorescence-labeled B-MSP-PMO and MSP-B-PMO conjugates indicates endocytosis is likely the mechanism for the cell uptake. Uptake is expressed as the median of cell fluorescence distribution in an experiment normalized to the cell fluorescence distribution median in untreated control (internalization at 37 °C). and shown as mean ± SEM. Significant cellular uptake decrease was observed in cells treated with low temperature, heparin and depletion of ATP compared with 37 °C for B-MSP-PMO and MSP-B-PMO conjugates (*$P < 0.001$, *t*-test, $n = 6$, *n* represents the number of biological replicates). MSP, muscle-targeting peptide; PMO, phosphorodiamidate oligomers.

conjugates in H2K *mdx* myoblasts showed that the difference in cell uptake was more pronounced at lower concentrations (**Figure 3b**), which is consistent with our previous report finding more striking differences in *in vivo* activity at lower dosages.[14] Furthermore, RT-PCR performed on RNA harvested from H2K *mdx* cells treated with different concentrations of fluorescein-labeled peptide-PMO conjugates showed that MSP-B-PMO was less effective at inducing exon-skipping than B-MSP-PMO, corroborating the above *in vivo* results and supporting the finding of greater uptake in B-MSP-PMO treated cells (**Figure 3b**,**c**,**d**). Moreover, the data suggests that B-MSP-PMO has over threefold increase in activity compared with MSP-B-PMO *in vitro*, and that these results appear to be due to the differences in muscle cell delivery efficiency (**Figure 3d**). Intriguingly, a significant but relatively small increase in cellular uptake appears to result in highly significant differences in exon-skipping activity, suggesting that small increases in delivery efficacy can be exponentially beneficial therapeutically.

The result in H2K *mdx* cells was then replicated in C2C12 myoblasts, mouse primary cardiomyocytes from C57BL/6 mice and HeLa cells treated with fluorescein-labeled B-MSP-PMO and MSP-B-PMO. Fluorescence activated cell sorting (FACS) was utilized for measuring the uptake of PMO conjugates in these different cell types and the increased uptake with B-MSP-PMO was evident in all tested cells with the exception of HeLa cells (**Figure 3e**). As expected, the uptake of both conjugates was dose-dependent in C2C12 (**Figure 3f**). Interestingly, the highest uptake was found in primary cardiomyocytes with both conjugates, suggesting that there exist no intrinsic barriers to cellular uptake and exon-skipping activity in primary cardiomyocytes. Therefore the low exon-skipping efficiency observed in heart in *mdx* mice with reported oligonucleotides can likely be attributed to relatively ineffective delivery to heart,[2–5] caused by an inability to cross the vascular endothelial layer, which is not assayed in the cell culture model.

Both B-MSP-PMO and MSP-B-PMO conjugates utilize similar cell uptake pathways

The findings from above studies support the hypothesis that increased muscle cell uptake is responsible for the enhanced exon-skipping activity of B-MSP-PMO. We therefore wished to characterize the cell uptake pathway of B-MSP-PMO in muscle cells. We initially studied the effects of ATP depletion and temperature on fluorescein-labeled B-MSP-PMO and MSP-B-PMO uptake in C2C12 myoblasts. C2C12 cells were incubated with fluorescein-labeled B-MSP-PMO and MSP-B-PMO for 1 hour, and the mean fluorescence level was evaluated using FACS analysis. As shown in **Figure 4**, the uptake of both peptide-PMO conjugates was significantly inhibited at 4 °C, with B-MSP-PMO and MSP-B-PMO reduced by 56 and 44%, respectively. When cells were preincubated with sodium azide and deoxyglucose to deplete the cellular ATP pool, a small but significant reduction in fluorescence levels of both peptide-PMO conjugates was also observed, with B-MSP-PMO and MSP-B-PMO showing 35 and 32% reduction, respectively (**Figure 4**). Dependence on both temperature and ATP levels is in line with an energy-dependent mechanism of B-MSP-PMO and MSP-B-PMO internalization in C2C12 cells, suggesting that endocytosis or other active transport is likely involved in the uptake of B-MSP-PMO and MSP-B-PMO in C2C12 cells. Since inhibiting endocytosis and energy-dependent process is detrimental for cells, incubations have been done for short times explicating the incomplete inhibition.

HSPG are found abundantly on the extracellular matrix[18] and could serve as binding sites for peptide PMO conjugates before cellular internalization. To evaluate the possible role of cell surface HSPGs on the uptake of fluorescein-labeled B-MSP-PMO and MSP-B-PMO, C2C12 cells were preincubated with heparin to compete with HSPGs binding on the cell surface. Significant inhibition was observed in both peptide-PMO conjugate uptake (**Figure 4**; 51% for B-MSP-PMO), albeit to a lesser extent with MSP-B-PMO (22%), suggesting that HSPGs at least partially mediate the uptake of both B-MSP-PMO and MSP-B-PMO. As inhibition of HSPGs appears to affect B-MSP-PMO to a greater degree than MSP-B-PMO, the difference in the way that these chimeric peptide conjugates interact with HSPGs may partially account for the observed differences in cellular uptake efficiency.

Discussion

AO-mediated exon-skipping therapeutics for DMD has garnered significant interest in the past decade, not solely for the potential benefits to patients with a devastating muscle-wasting disease,[1–7,10] but also as a model system for the development of other AO-based therapeutics. Unlike small molecule drugs, nucleic acid therapeutic compounds and their analogues are typically noncell-permeable,[2,19] and therefore overcoming the barrier of cell delivery is critical for developing these compounds as therapeutic agents. In addition, due to the high costs of production and potential for undesirable side effects, specific cell targeting is crucial to clinical success. Hence, the development of universally applicable modalities for effective systemic delivery of AOs and improved cell uptake will be of great benefit to the gene therapy field. We have previously shown that the B peptide conjugated to an exon-skipping PMO greatly enhances cellular uptake after systemic administration in *mdx* mice.[5] Moreover, the addition of a muscle-targeting motif improves PMO uptake significantly, in an order-dependent manner.[14] This raises the questions of whether the improved uptake efficiency due to the relative order of a cell-targeting peptide and cell-penetrating peptide is a general phenomenon or specific to each peptide and what the mechanism of cell uptake is for these chimeric peptides. In this study, we showed differential exon-skipping efficiency *in vivo* using another muscle-targeting peptide (B-9-PMO) compared with its reverse order analogue 9-B-PMO, but the same effect was not observed with a control nonmuscle targeting peptide (peptide 3). Higher exon skipping was seen with B peptide placed at the free end of the chimeric peptide conjugate with both MSP and peptide 9, but not with nonmuscle targeting peptide 3, implying the importance of this muscle-targeting motif structure for improving exon-skipping efficiency. This improved exon-skipping effect was shown to be likely due to increased cellular uptake both *in vivo* and *in vitro* and was also demonstrated to be partially dependent on ATP, temperature and surface HSPG in C2C12 cells. However, the general applicability of this design will merit further investigation.

The dependence on energy for cell uptake and the lack of hydrophobic domains within the chimeric peptide-PMO compounds rules out the possibility of direct diffusion of the peptide conjugates across the cell membrane. The requirement for ATP energy suggests that uptake was mediated by either endocytosis or other active transport mechanism. As the B peptide is arginine-rich, its likely uptake mechanism is suggested by studies of other CPPs in this class. Numerous studies with Tat (*trans*-activator of transcription – discovered in the basic region of HIV-1 Tat protein) and penetratin (derived from helix 3 of the Antennapedia homeodomain protein from *Drosophila melanogaster*) arginine-rich peptides conjugated to a variety of cargoes have shown these peptides to be dependent on endocytosis.[20] Most arginine-rich peptides (R9, Tat and penetratin), particularly Tat, are also dependent on HSPGs for cellular uptake.[21–24] Hence, it is no surprise that our finding shows HSPGs likely play a role in the uptake of chimeric PMO conjugates containing the B peptide. Although direct binding of arginine-rich peptides to HSPGs has been demonstrated[19] and HSPGs have been shown to carry cargos into intracellular vesicles,[25] multiple endocytic pathways have been implicated in the uptake of arginine-rich peptides.[19] This suggests a possible internalization mechanism whereby chimeric peptide PMOs bind transiently to negatively charged HSPGs at the cell surface and are subsequently taken up into cells as the HSPGs are internalized through nonspecific endocytic processes. Therefore, our preliminary mechanistic evidence suggests that uptake of chimeric PMO conjugates is likely via endocytosis though other active transport mechanisms cannot be excluded.

The importance of structural alignment of peptide motifs within the chimeric peptide-PMO conjugates suggests that steric restriction is a possible reason for the reduced activity of MSP-B peptide. Our data indicated the order-specific effects observed with B-MSP and B-9 vs. other combinations e.g., MSP-B, which provides insight for the future design of effective muscle-specific chimeric peptides. Furthermore, evidence from *in vitro* and *in vivo* studies e.g., cellular uptake and biodistribution, showed that the improved exon-skipping activity of B-MSP-PMO is due to the increased muscle cell uptake and internalization. Although the difference in cellular uptake in C2C12 cells between B-MSP-PMO and MSP-B-PMO was marginal at 1 μmol/l and became significant at lower concentrations (i.e., 500 and 300 nmol/l), the effects on exon skipping were much more pronounced as shown in **Figure 3**. The disparity between the cellular uptake and the resultant activity

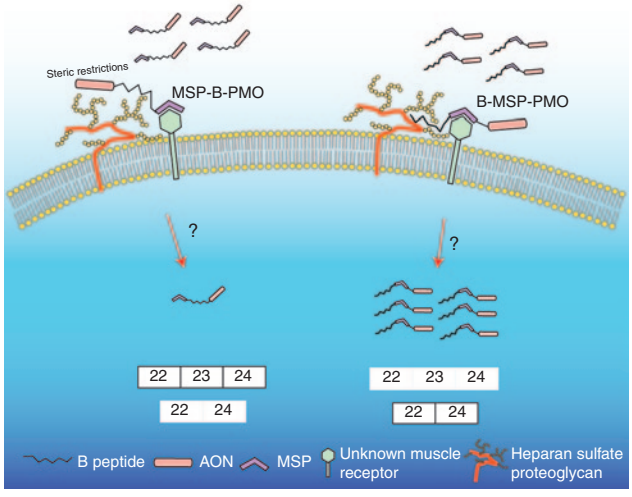

Figure 5 Schematic for the uptake mechanism hypothesis. The muscle-specific peptide (MSP) is hypothesized to have a low affinity for an unknown cell surface marker on muscle cells that can be enhanced by the interaction of the B peptide with heparan sulfate proteoglycans and lipid bilayer. The interaction may require insertion of the B peptide into the HSPG complex. This enhancement allows the PMO to reside on the surface long enough to be taken up by endocytosis into the cell. The affinity of B peptide for HSPGs may explain the efficiency of uptake of B-PMO *in vivo*. If MSP is placed before the B peptide, the B peptide–HSPG interaction is blocked sterically and only the weak MSP interaction is able to facilitate low levels of uptake. Numbers 22, 23 and 24 represent the *dystrophin* gene exons 22, 23 and 24, respectively. HSPG, heparan sulfate proteoglycans; PMO, phosphorodiamidate oligomers.

observed is possibly due to a difference in endosomal escape as most of the internalized peptide-cargo is potentially entrapped in endosomal compartments as reported previously.[26] Hence, we propose a model of PMO uptake when conjugated to a chimeric peptide comprising the B peptide and a cell-targeting peptide in which the peptide motif order modulates the affinity of B peptide for HSPGs on the cell surface of specific cell types (**Figure 5**).

Materials and methods

Animals. Six- to eight-week old *mdx* mice were used in all experiments (four mice each in the test and control groups). The experiments were carried out in the Animal unit, Department of Physiology, Anatomy and Genetics, University of Oxford, Oxford, UK according to procedures authorized by the UK Home Office under the project license 30/2652. Mice were killed by CO_2 inhalation or cervical dislocation at desired time points, and muscles and other tissues were snap-frozen in liquid nitrogen-cooled isopentane and stored at –80 °C.

PMO and peptide-PMO conjugates. PMO and peptide-PMO conjugates used in the study are listed in **Table 1**. PMO M23D is a 25 mer PMO targeting the boundary sequences of exon and intron 23 of the mouse *dystrophin* gene. Conjugations of peptides with PMO were synthesized by a stable amide linker.[27] All conjugates were synthesized by AVI Biopharma Inc. (Corvallis, OR; currently Sarepta). For systemic intravenous injections, PMO-peptide conjugates in 80 µl saline buffer were injected into tail vein of *mdx* mice at the final dose of 25 mg/kg. For tissue distribution experiments, treated *mdx* mice were subjected to perfusion before the tissues were harvested. Firstly, *mdx* mice were deeply anesthetized with pentobarbitone intraperitoneally until mice were unconscious (but not dead). Then an incision was made through abdomen the length of the diaphragm to expose the heart (the heart should be still beating). A needle was placed into the left ventricle and the right atrium was cut immediately and subsequently a minimum of three-times volume of blood volume of cold PBS was used for perfusion until the liver became a light coffer color.

RNA extraction and nested RT-PCR analysis. Total RNA was extracted with TRIzol (Invitrogen, Paisley, UK) and 200 ng of RNA template was used for 20 µl RT-PCR with OneStep RT-PCR kit (Qiagen, UK). The primer sequences for the initial RT-PCR were Exon20Fo 5′-CAGAATTCTGCCAATTGCTGAG-3′ and Ex26Ro 5′-TTCTTCAGCTTGTGTCATCC-3′ for amplification of messenger RNA from exons 20 to 26. The cycle conditions were 95 °C for 30 seconds, 55 °C for 1 minute and 72 °C for 2 minutes for 25 cycles. RT-PCR product (1 µl) was then used as the template for secondary PCR performed in 25 µl with 0.5 U Taq DNA polymerase (Invitrogen). The primer sequences for the second round were Ex20Fi 5′-CCCAGTCTACCACCCTATCAGAGC-3′ and Ex24Ri 5′-CAGCCATCCATTTCTGTAAGG -3′. The cycle conditions were 95 °C for 1 minute, 57 °C for 1 minute, and 72 °C for 2 minutes for 25 cycles. The products were examined by electrophoresis on a 2% agarose gel.

Immunohistochemistry and histology. Series of 8 µm sections were examined for dystrophin expression with rabbit polyclonal antibody from Abcam (ab152777, Cambridge, MA) as described.[5] For dystrophin-positive fiber counting, the maximum number of dystrophin-positive fibers in one section was counted using the fluorescence microscope and the muscle fibers were defined as dystrophin-positive when more than two thirds of the single fiber showed continuous staining.

Measurement of labeled peptide-PMO conjugates in tissues. Fifty micrograms of tissues taken from treated and untreated control *mdx* mice were homogenized in 350-µl digestion buffer and lysed in a shaking incubator for 16 hour at 60 °C. After incubation, the supernatant were collected for the assay. A standard curve of each compound was established using lysis buffer and serially diluted the compound into the concentration range from 1 µmol/l to 5 pmol/l, then incubated the solution in dark room for 16 hours at 60 °C. Bradford assay was used for measuring the protein concentration of lysed samples, 100 µl solution was applied for the measurement with 90 µl sample buffer and 10 µl 100 mmol/l Na_2HCO_3 (pH 9.5) to increase the sensitivity. The maximal excitation wavelength of 495 nm and the maximal emission wavelength of 524 nm were used for fluorescence measurement. The detection limit and linear range of each compound was determined with the standard curve and normalized by the blank. Tissues from untreated *mdx* control mice were used for determining the background auto-fluorescence. Fluorescence of peptide-PMOs for a given tissue = fluorescence of the tissue – the background auto-fluorescence of that tissue at the same protein concentration. In addition, the concentration of PMO can be expressed as ng/mg of tissue.

Cell transfection and confocal microscopy. H2K *mdx* myoblasts were cultured as previously reported.[8] In brief, cells were cultured at 33 °C in 10% CO_2 in Dulbecco's Modified Eagle's Medium supplemented with 20% fetal calf serum, 2% chicken embryo extract (PAA Laboratories Ltd, Yeovil, UK), and 20 units ml^{-1} γ-interferon (Roche, Hertfordshire, UK). Cells were then treated with trypsin and plated at 2×10^4 cells per well in 24-well plates coated with 200 µg/ml gelatine (Sigma). H2K *mdx* cells were transfected 24 hours with peptide-PMO conjugates after trypsin treatment in a final volume of 0.5 ml supplemented medium. Immediately prior to examination of transfected cells, growth medium was removed from the wells and the cells were washed with PBS three-times. Fresh growth medium was then added to the cells. The cells were then examined using a LSM 510 META inverted fluorescence confocal microscope (Carl Zeiss International, Cambridge, UK). HeLa pLuc705 cells (a generous gift from Dr. R. Kole) and mouse myoblast cell line (C2C12 – ATCC: CRL-1772) were cultured in Dulbecco's Modified Eagle's Medium (Gibco, Paisley, UK) supplemented with 10% fetal bovine serum (Biowest), 1% Na pyruvate (Gibco), 1% nonessential amino acids (Gibco) and 1% penicillin-streptomycin-neomycin (Gibco).

Neonatal cardiac cells were isolated from 1- to 2-day-old C57BL/6 mice (Charles River) ventricles by digestion with type 4 collagenase (Serlabo) and pancreatin (Gibco). Animals were killed in conformity with the Guide for the Care and Use of Laboratory Animals published by the NIH

(Publication No. 85-23). Freshly isolated cells were seeded in 90-mm Petri dishes to allow selective adhesion of cardiac fibroblasts[27] in plating medium: 250 ml Dulbecco's Modified Eagle's Medium (Gibco), 250 ml M199 (Sigma–Aldrich), 5 ml glutamine – PS 100×, 50 ml horse serum (10%), 25 ml fetal bovine serum (5%). Thereafter, cardiomyocytes were decanted from the plates and seeded in wells coated with 0.1% gelatin (Sigma–Aldrich).

Cellular uptake and endocytosis analysis. To analyze the internalization of fluorescein-labeled peptide-PMO conjugates by FACS, 2×10^5 cells were plated in 12-well plate and cultured overnight. The cultured medium was discarded, and the cells were washed with PBS. PBS was discarded and the cells were incubated with 1-µmol/l peptide-PMO conjugates in OptiMEM. After 1 hour of incubation at 37 °C, the cells were washed twice with PBS, treated with trypsin (0.5 mg/ml)/EDTA.4Na (0.35 mmol/l; 5 minutes at 37 °C), resuspended in PBS 5% fetal calf serum, centrifuged at 900×*g* (5 minutes, 4 °C) and resuspended in PBS 0.5% fetal calf serum containing 0.05 µg/ml propidium iodide (Molecular Probes, Paisley, UK). Fluorescence analysis was performed with FACS fluorescence activated sorter (BD Bioscience, Oxford, UK). Cells stained with PI were excluded from further analysis. A minimum of 10,000 events per sample was analyzed.

For the 4 °C condition, the cells were preincubated with OptiMEM 1 hour at 4 °C and then incubated with 1 µmol/l peptide-PMO conjugated in OptiMEM for 1 hour at 4 °C. For the ATP-depletion condition, the cells were preincubated with 10 mmol/l sodium azide and 6 mmol/l 2-deoxy-D-glucose in OptiMEM 1 hour at 37 °C and then incubated with 1-µmol/l peptide-PMO conjugates in OptiMEM with 10 mmol/l sodium azide and 6 mmol/l 2-deoxy-D-glucose for 1 hour at 37 °C. For the HSPG-inhibiting condition, the cells were preincubated with 50 µg/ml heparin in OptiMEM 1 hour at 37 °C and then incubated with 1 µmol/l peptide-PMO conjugated in OptiMEM with 50 µg/ml heparin for 1 hour at 37 °C. Subsequently, the cells were trypsinizated and prepared for FACS measurements as described above.

Protein extraction and western blot. Protein extraction and western blot were carried out as previously described.[5] Various amounts protein from normal C57BL/6 mice as a positive control and corresponding amounts of protein from muscles of treated or untreated *mdx* mice were used. The membrane was probed with DYS1 (monoclonal antibody against dystrophin R8 repeat, 1:200, NovoCastra, Newcastle upon Tyne, UK) for the detection of dystrophin protein. The bound primary antibody was detected by horseradish peroxidase-conjugated rabbit anti-mouse IgGs and the ECL western blotting analysis system (Amersham Pharmacia Biosciences, Amersham, UK). The intensity of the bands obtained from treated *mdx* muscles was measured by Image J software; the quantification is based on band intensity and area, and is compared with that from normal muscles of C57BL/6 mice.

Statistical analysis. All data are reported as mean values ± SEM. Statistical differences between treatment groups and control groups were evaluated by SigmaStat (Systat Software, UK) and two-tailed Student's *t* test was applied.

Supplementary material

Figure S1. Systemic administration of 3-B-PMO and B-3-PMO conjugates in young *mdx* mice at 25 mg/kg dose.

Acknowledgments. This work was supported by research grants from Action Duchenne to M.J.A.W and National Natural Science Foundation of China (No.81071443), Chinese National Basic Research Program (973) (No. 2012CBA01305, 2012CB932503), Research Fund for the Doctoral Program of Higher Education of China (Grant No. 20111202110002) and Program for New Century Excellent Talents (NCET-10–0957) to H.F.Y. The authors acknowledge Professor Kay Davies (Department of Physiology, Anatomy and Genetics, University of Oxford) for providing access to facilities including the *mdx* mouse colony.

Conflict of interest. The authors declare no competing financial or other conflicts of interest.

1. Wood, MJ, Gait, MJ and Yin, H (2010). RNA-targeted splice-correction therapy for neuromuscular disease. *Brain* **133**(Pt 4): 957–972.
2. Lu, QL, Rabinowitz, A, Chen, YC, Yokota, T, Yin, H, Alter, J *et al.* (2005). Systemic delivery of antisense oligoribonucleotide restores dystrophin expression in body-wide skeletal muscles. *Proc Natl Acad Sci USA* **102**: 198–203.
3. Alter, J, Lou, F, Rabinowitz, A, Yin, H, Rosenfeld, J, Wilton, SD *et al.* (2006). Systemic delivery of morpholino oligonucleotide restores dystrophin expression bodywide and improves dystrophic pathology. *Nat Med* **12**: 175–177.
4. Yokota, T, Lu, QL, Partridge, T, Kobayashi, M, Nakamura, A, Takeda, S *et al.* (2009). Efficacy of systemic morpholino exon-skipping in Duchenne dystrophy dogs. *Ann Neurol* **65**: 667–676.
5. Yin, H, Moulton, HM, Seow, Y, Boyd, C, Boutilier, J, Iverson, P *et al.* (2008). Cell-penetrating peptide-conjugated antisense oligonucleotides restore systemic muscle and cardiac dystrophin expression and function. *Hum Mol Genet* **17**: 3909–3918.
6. Goemans, NM, Tulinius, M, van den Akker, JT, Burm, BE, Ekhart, PF, Heuvelmans, N *et al.* (2011). Systemic administration of PRO051 in Duchenne's muscular dystrophy. *N Engl J Med* **364**: 1513–1522.
7. Cirak, S, Arechavala-Gomeza, V, Guglieri, M, Feng, L, Torelli, S, Anthony, K *et al.* (2011). Exon skipping and dystrophin restoration in patients with Duchenne muscular dystrophy after systemic phosphorodiamidate morpholino oligomer treatment: an open-label, phase 2, dose-escalation study. *Lancet* **378**: 595–605.
8. Yin, H, Lu, Q and Wood, M (2008). Effective exon skipping and restoration of dystrophin expression by peptide nucleic acid antisense oligonucleotides in mdx mice. *Mol Ther* **16**: 38–45.
9. Wu, B, Lu, P, Benrashid, E, Malik, S, Ashar, J, Doran, TJ *et al.* (2010). Dose-dependent restoration of dystrophin expression in cardiac muscle of dystrophic mice by systemically delivered morpholino. *Gene Ther* **17**: 132–140.
10. Wu, B, Moulton, HM, Iversen, PL, Jiang, J, Li, J, Li, J *et al.* (2008). Effective rescue of dystrophin improves cardiac function in dystrophin-deficient mice by a modified morpholino oligomer. *Proc Natl Acad Sci USA* **105**: 14814–14819.
11. Jearawiriyapaisarn, N, Moulton, HM, Buckley, B, Roberts, J, Sazani, P, Fucharoen, S *et al.* (2008). Sustained dystrophin expression induced by peptide-conjugated morpholino oligomers in the muscles of mdx mice. *Mol Ther* **16**: 1624–1629.
12. Wu, B, Li, Y, Morcos, PA, Doran, TJ, Lu, P and Lu, QL (2009). Octa-guanidine morpholino restores dystrophin expression in cardiac and skeletal muscles and ameliorates pathology in dystrophic mdx mice. *Mol Ther* **17**: 864–871.
13. Samoylova, TI and Smith, BF (1999). Elucidation of muscle-binding peptides by phage display screening. *Muscle Nerve* **22**: 460–466.
14. Yin, H, Moulton, HM, Betts, C, Seow, Y, Boutilier, J, Iverson, PL *et al.* (2009). A fusion peptide directs enhanced systemic dystrophin exon skipping and functional restoration in dystrophin-deficient mdx mice. *Hum Mol Genet* **18**: 4405–4414.
15. Yin, H, Moulton, HM, Betts, C, Merritt, T, Seow, Y, Ashraf, S *et al.* (2010). Functional rescue of dystrophin-deficient mdx mice by a chimeric peptide-PMO. *Mol Ther* **18**: 1822–1829.
16. Seow, Y, Yin, H and Wood, MJ (2010). Identification of a novel muscle targeting peptide in mdx mice. *Peptides* **31**: 1873–1877.
17. Yin, H, Saleh, AF, Betts, C, Camelliti, P, Seow, Y, Ashraf, S *et al.* (2011). Pip5 transduction peptides direct high efficiency oligonucleotide-mediated dystrophin exon skipping in heart and phenotypic correction in mdx mice. *Mol Ther* **19**: 1295–1303.
18. Guterstam, P, Madani, F, Hirose, H, Takeuchi, T, Futaki, S, El Andaloussi, S *et al.* (2009). Elucidating cell-penetrating peptide mechanisms of action for membrane interaction,

cellular uptake, and translocation utilizing the hydrophobic counter-anion pyrenebutyrate. *Biochim Biophys Acta* **1788**: 2509–2517.
19. Turnbull, J, Powell, A and Guimond, S (2001). Heparan sulfate: decoding a dynamic multifunctional cell regulator. *Trends Cell Biol* **11**: 75–82.
20. Lebleu, B, Moulton, HM, Abes, R, Ivanova, GD, Abes, S, Stein, DA *et al.* (2008). Cell penetrating peptide conjugates of steric block oligonucleotides. *Adv Drug Deliv Rev* **60**: 517–529.
21. Sadoshima, J and Izumo, S (1993). Molecular characterization of angiotensin II–induced hypertrophy of cardiac myocytes and hyperplasia of cardiac fibroblasts. Critical role of the AT1 receptor subtype. *Circ Res* **73**: 413–423.
22. Melikov, K and Chernomordik, LV (2005). Arginine-rich cell penetrating peptides: from endosomal uptake to nuclear delivery. *Cell Mol Life Sci* **62**: 2739–2749.
23. Richard, JP, Melikov, K, Brooks, H, Prevot, P, Lebleu, B and Chernomordik, LV (2005). Cellular uptake of unconjugated TAT peptide involves clathrin-dependent endocytosis and heparan sulfate receptors. *J Biol Chem* **280**: 15300–15306.
24. Ziegler, A, Nervi, P, Dürrenberger, M and Seelig, J (2005). The cationic cell-penetrating peptide CPP(TAT) derived from the HIV-1 protein TAT is rapidly transported into living fibroblasts: optical, biophysical, and metabolic evidence. *Biochemistry* **44**: 138–148.
25. Console, S, Marty, C, García-Echeverría, C, Schwendener, R and Ballmer-Hofer, K (2003). Antennapedia and HIV transactivator of transcription (TAT) "protein transduction domains" promote endocytosis of high molecular weight cargo upon binding to cell surface glycosaminoglycans. *J Biol Chem* **278**: 35109–35114.
26. Mäe, M, Andaloussi, SE, Lehto, T and Langel, U (2009). Chemically modified cell-penetrating peptides for the delivery of nucleic acids. *Expert Opin Drug Deliv* **6**: 1195–1205.
27. Wu, RP, Youngblood, DS, Hassinger, JN, Lovejoy, CE, Nelson, MH, Iversen, PL *et al.* (2007). Cell-penetrating peptides as transporters for morpholino oligomers: effects of amino acid composition on intracellular delivery and cytotoxicity. *Nucleic Acids Res* **35**: 5182–5191.

Supplementary Information accompanies this paper on the Molecular Therapy–Nucleic Acids website (http://www.nature.com/mtna)